PARAMETRIC ADAPTIVE SIGNAL DETECTION FOR HYPERSPECTRAL IMAGING

Hongbin Li
ECE Department, Stevens Institute of Technology
Hoboken, NJ 07030, USA
E-mail: hli@stevens.edu

James H. Michels
JHM Technologies, Box 4142
Ithaca, NY 14852-4142, USA
E-mail: jmichels@americu.net

***Abstract*— In this paper, we introduce a class of *training-efficient* adaptive signal detectors that exploit a parametric model taking into account the *non-stationarity* of HSI data in the spectral dimension. A maximum likelihood (ML) estimator is presented for estimation of the parameters associated with the proposed parametric model. Several important issues are discussed, including model order selection, training screening, and time-series based whitening and detection, which are intrinsic parts of the proposed parametric adaptive detectors. Experimental results using real HSI data reveal that the proposed parametric detectors are more training-efficient and outperform conventional covariance-matrix based detectors when the training size is limited.**

I. INTRODUCTION

Hyperspectral imaging (HSI) has numerous civilian and military applications [1]. A challenging problem in HSI applications is the so-called *subpixel target detection*, which involves detecting objects occupying only a portion of a full pixel [2]. The signal produced by the HSI sensors consists of both the *object* and *background*, the latter behaving effectively as interference. The problem is reminiscent of that of detecting a known signal with unknown amplitude in colored noise with unknown correlation. A multitude of solutions have been developed, including the Kelly's generalized likelihood ratio test (GLRT), adaptive matched filter (AMF), adaptive coherence estimator (ACE), among others (see [2] and references therein). While these detectors can be applied to the HSI subpixel target detection problem, there is a major difficulty when training is limited. In particular, the above *covariance-matrix based detectors* rely on an estimate of the background covariance matrix, which is obtained from *target-free* training pixels. The size of the background covariance matrix is identical to the number of spectral bands that is typically in the order of hundreds. A good estimate of the covariance matrix would require several hundred or more target-free training pixels, which may not be available in heterogeneous or dense-target environments.

In this paper, we present a class of parametric adaptive detectors, which utilize a parametric model for the background of the HSI data to achieve training efficiency. Our approach builds on earlier parametric detectors, in particular, the parametric adaptive matched filter (PAMF) [3], [4] developed for space-time adaptive processing (STAP) in airborne radars. The major difference is that whereas the PAMF detector is based on stationary autoregressive (AR) models that are appropriate for radar applications, we have to deal with non-stationarity of HSI data in the spectral dimension, and employ a non-stationary (NS) AR model for our problem. Along with the proposed NS-AR model based detectors, we address several important issues including parameter estimation, model order selection, and training screening.

II. DATA MODEL AND PROBLEM STATEMENT

Each pixel in an HSI data cube [2] can be represented as an $L \times 1$ *real-valued* vector: $\boldsymbol{x} = [x(0), x(1), \ldots, x(L-1)]^T$, where L is the total number of spectral bands, $x(l)$ is the spectral response at the lth spectral band, and $(\cdot)^T$ denotes transpose. HSI data usually has non-zero mean [2]. A de-meaning process is often used to remove the sample mean estimated from the neighbor pixels. The *subpixel signal detection* problem is described by [2]

$$\begin{aligned} H_0: &\quad \boldsymbol{x} = \boldsymbol{b}, && \text{target absent} \\ H_1: &\quad \boldsymbol{x} = a\boldsymbol{s} + \boldsymbol{b}, && \text{target present} \end{aligned} \tag{1}$$

where $\boldsymbol{x} \in \mathbb{R}^{L\times 1}$ is the de-meaned test pixel, $\boldsymbol{s} \in \mathbb{R}^{L\times 1}$ is the *signature vector* of the target object, which is assumed known, with *unknown* amplitude a, and $\boldsymbol{b} \in \mathbb{R}^{L\times 1}$ denotes the background plus system noise, which is modeled as a Gaussian[1] random vector with zero mean and an unknown covariance matrix $\boldsymbol{R}_b$ [2]. Like [2], we assume the availability of N training pixels $\boldsymbol{x}_1, \ldots, \boldsymbol{x}_N$, which are independent and identically distributed (i.i.d.) Gaussian random vectors with zero mean and covariance matrix $\boldsymbol{R}_b$, and independent of the text pixel $\boldsymbol{x}$. In surveillance applications when the target class is rare or sparsely populated, the training pixels are usually taken as those surrounding the test pixel and assumed target-free [2].

The problem is to find an efficient decision rule for the composite hypothesis testing problem (1), given knowledge of the test pixel $\boldsymbol{x}$, target signal signature $\boldsymbol{s}$, and training pixels $\boldsymbol{x}_1, \ldots, \boldsymbol{x}_N$.

III. PROPOSED APPROACH

We present herein a class of parametric adaptive signal detectors with reduced training requirement. The proposed detectors, detailed in Section III-B, rely on an NS-AR model introduced in Section III-A, an ML parameter estimation algorithm derived in Section III-C, a model order selection method discussed in Section III-D, and a training screening technique presented in Section III-E.

A. NS-AR Modeling

Since HSI data is non-stationary (NS) across the spectral dimension [6], standard parametric AR models for stationary processes are not applicable. However, approximate stationarity is still retained over a sufficiently small number of adjacent spectral bands [6]. In the following, we consider an NS-AR modeling approach by taking into account such *local stationarity* of HSI data. Specifically, let $x_n(l)$ denote the spectral response at the lth spectral band of the nth training pixel $\boldsymbol{x}_n$. We slice $\boldsymbol{x}_n$ into into $L - L_s + 1$ overlapping subvectors: $\boldsymbol{x}_{n,l} \triangleq [x_n(l), \ldots, x_n(l + L_s - 1)]^T$, $l = 0, \ldots, L - L_s$, where $L_s \leq L$ denotes the length of the subvectors. For sufficiently small L_s, each subvector $\boldsymbol{x}_{n,l}$ can be modeled as an Mth-order AR process:

$$\begin{aligned} x_n(k) = -\textstyle\sum_{m=1}^{M} a_l(m) x_n(k-m) + w_{n,l}(k), \\ k = l, l+1, \ldots, l + L_s - 1;\ n = 1, \ldots, N, \end{aligned} \tag{2}$$

where $w_{n,l}(k)$ denotes the modeling residual for the lth subvector $\boldsymbol{x}_{n,l}$. The residual is Gaussian (since $x_n(k)$ is so) with zero-mean and variance σ_l^2, and spectrally white so that $\{w_{n,l}(k)\}$ are independent with respect to k and n. Note that the lth set of the AR coefficients, $a_l(1), \ldots, a_l(M)$, is associated with the lth subvector $\boldsymbol{x}_{n,l}$, and that different subvectors are associated with different sets of AR

This work was supported by the Air Force Research Laboratory (AFRL) Visiting Faculty Research Program (VFRP).

[1] A Gaussian model might not be fully appropriate for some HSI data, and alternative modeling approaches are available [5].

coefficients. For simplicity, we consider an AR model of fixed model order M. From the estimation perspective, the choice of M and window size L_s should be made with tradeoffs among the bias, variance and stationarity of the modeling approach [5]. From the application aspect, these parameters are related to the HSI sensor characteristics. For the HSI data used in this paper, we found that a window size $8 \leq L_s \leq 15$ is generally appropriate for modeling. Once L_s is selected, we can use information criterion based model order selection techniques to determine M. We leave the details to Section III-D.

B. NS-AR Model Based Parametric Adaptive Detectors

Given the above NS-AR model (2) for target-free HSI data (i.e., the background), a time-series based (as opposed to the covariance-matrix based) whitening process can be developed without explicitly estimating $\boldsymbol{R}_b$. This leads to a class of parametric adaptive detectors that are summarized below:

- **Step 1** (*Parameter Estimation*): Estimate $\{a_l(m)\}$ and $\{\sigma_l^2\}$ in (2) from the training $\{\boldsymbol{x}_n\}_{n=1}^N$ by using an ML based estimator detailed in Section III-C. Let $\{\hat{a}_l(m), \hat{\sigma}_l^2\}$ denote the estimates.
- **Step 2** (*Whitening*): Perform whitening as follows:

$$\begin{aligned} \breve{x}(l) &= \frac{1}{\hat{\sigma}_l}\left[x(l) + \textstyle\sum_{m=1}^{M} \hat{a}_{l-L_s}(m)x(l-m)\right], \\ \breve{s}(l) &= \frac{1}{\hat{\sigma}_l}\left[s(l) + \textstyle\sum_{m=1}^{M} \hat{a}_{l-L_s}(m)s(l-m)\right], \end{aligned} \tag{3}$$

  where $\breve{x}(l)$ and $\breve{s}(l)$ are the lth output sample of the whitening filter, $l = L_s - 1, \ldots, L-1$, when the input is test pixel $\boldsymbol{x}$ and target signature $\boldsymbol{s}$, respectively. Note from (3) that each set of the NS-AR parameter estimates, i.e., $\{\hat{a}_l(m)\}_{m=1}^M$ and $\hat{\sigma}_l$, is used to compute only one pair of output samples $\breve{x}(l)$ and $\breve{s}(l)$.
- **Step 3** (*Detection*): The outputs of the shift-varying whitening filter can be used to form a decision statistic. Based on how the decision statistic is formed, we have various (a class of) parametric detectors. For example, the parametric counterpart of the covariance-matrix based ACE [2] detector is

$$\frac{\left|\sum_{l=L_s-1}^{L-1} \breve{s}(l)\breve{x}(l)\right|^2}{\left(\sum_{l=L_s-1}^{L-1} \breve{s}^2(l)\right)\left(\sum_{l=L_s-1}^{L-1} \breve{x}^2(l)\right)} \underset{H_0}{\overset{H_1}{\gtrless}} t_{\text{NS-NPAMF}}, \tag{4}$$

  which is referred to as the *NS-NPAMF* detector, since it is also an NS version of the normalized PAMF (NPAMF) detector [7]. An NS-AR model based AMF or Kelly test can be obtained in a similar fashion [5].

Note that the above NS-NPAMF detector reduces to the NPAMF detector, when $L_s = L$, that is, the sliding window reaches the maximum value and includes the entire spectral bands. In that case, the NS-AR model in (2) reduces to the standard stationary AR model.

C. ML Estimation of NS-AR Coefficients

The least-squares (LS) estimator for the NS-AR model introduced in [6] is shown to be equivalent to an ML based estimator in [5], which is presented next. Let $\boldsymbol{x}_{n,l} \triangleq [x_n(l+M), \ldots, x_n(l+L_s-1)]^T$ and

$$\boldsymbol{X}_{n,l} \triangleq \begin{bmatrix} x_n(l+M-1) & \ldots & x_n(l) \\ \vdots & \vdots & \vdots \\ x_n(l+L_s-2) & \ldots & x_n(l+L_s-M-1) \end{bmatrix}. \tag{5}$$

Then, the ML estimates are given by

$$\hat{\boldsymbol{a}}_l = -\left(\textstyle\sum_{n=1}^{N} \boldsymbol{X}_{n,l}^T \boldsymbol{X}_{n,l}\right)^{-1}\left(\textstyle\sum_{n=1}^{N} \boldsymbol{X}_{n,l}^T \boldsymbol{x}_{n,l}\right), \tag{6}$$

$$\hat{\sigma}_l^2 = [N(L_s - M)]^{-1}(\boldsymbol{x}_l^T \boldsymbol{P}_{\boldsymbol{X}_l}^{\perp} \boldsymbol{x}_l), \tag{7}$$

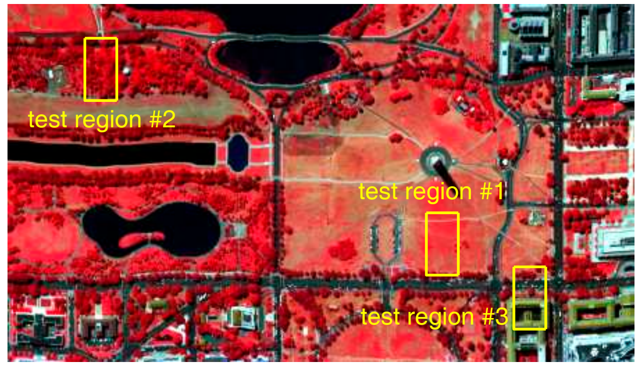

Fig. 1. HSI image of the Washington DC Mall with L=191 spectral bands. Three test regions are highlighted in yellow.

where $\boldsymbol{X}_l \triangleq [\boldsymbol{X}_{1,l}^T, \ldots, \boldsymbol{X}_{N,l}^T]^T$, $\boldsymbol{x}_l \triangleq [\boldsymbol{x}_{1,l}^T, \ldots, \boldsymbol{x}_{N,l}^T]^T$, $l = 0, 1, \ldots, L - L_s$, and $\boldsymbol{P}_{\boldsymbol{X}_l}^{\perp}$ is the projection matrix onto the null space of $\boldsymbol{X}_l$: $\boldsymbol{P}_{\boldsymbol{X}_l}^{\perp} = \boldsymbol{I} - \boldsymbol{X}_l\left(\boldsymbol{X}_l^T \boldsymbol{X}_l\right)^{-1} \boldsymbol{X}_l^T$, where $\boldsymbol{I}$ is an identity matrix.

D. NS-AR Model Order Selection

Model order selection for parametric models is a classical topic and has been investigated by various researchers for various models (e.g., [8]). We examine selecting an appropriate model for the NS-AR model in (2), which has not been addressed elsewhere. Although in principle it is possible to select a different M for each subvector $\boldsymbol{x}_{n,l}$, $l = 0, \ldots, L-L_s$, by a separate fitting of M to the information criterion, this is a tedious process. In the following, we use a fixed M for all l. Specifically, we consider a *generalized Akaike information criterion (GAIC)*, which chooses the model order M that minimizes

$$W(M) = \textstyle\sum_{l=0}^{L-L_s} \left[V_l(M) + \gamma(M)\right], \tag{8}$$

where $V_l(M)$ is the minimum cost (i.e., likelihood function) associated with the lth set of subvectors $\boldsymbol{x}_{1,l}, \ldots, \boldsymbol{x}_{N,l}$, and $\gamma(M)$ is a penalty term that penalizes increasing model order [8]. The minimum cost is [5]

$$V_l(M) = \frac{1}{2}N(L_s - M)[1 + \ln(2\pi)] + \frac{1}{2}N(L_s - M)\ln\hat{\sigma}_l^2(M), \tag{9}$$

where $\hat{\sigma}_l^2(M)$ is given by (7) and the dependence on M is made explicit. The penalty term typically takes the form [8]

$$\gamma(M) = \alpha(M+1)\ln(NL_s), \tag{10}$$

or

$$\gamma(M) = \alpha(M+1)\ln\left[\ln(NL_s)\right], \tag{11}$$

where $M + 1$ is the total number of unknowns for each set of subvectors $\{\boldsymbol{x}_{n,l}\}_{n=1}^N$, NL_s is the number of data samples contained in $\{\boldsymbol{x}_{n,l}\}_{n=1}^N$, and $\alpha \geq 2$ is a parameter of user choice. Note that the above GAIC reduces to the standard AIC when the $(L-L_s+1)$-term summation in (8) vanishes and $\gamma(M) = 2(M+1)$. It is known that AIC is not a consistent model order estimator. Choosing a penalty term proportional to $\ln(NL_s)$ or $\ln\left[\ln(NL_s)\right]$ is an effective way of obtaining a consistent order estimate [8].

E. Training Screening

One assumption made in Section II is that the N training pixels $\boldsymbol{x}_1, \ldots, \boldsymbol{x}_N$ are target-free. Training screening to eliminate "bad" training data for detection in *heterogeneous* or *dense-target* environments has been examined in a number of recent studies for radar target detection (e.g., [9]). We discuss here screening of heterogeneous

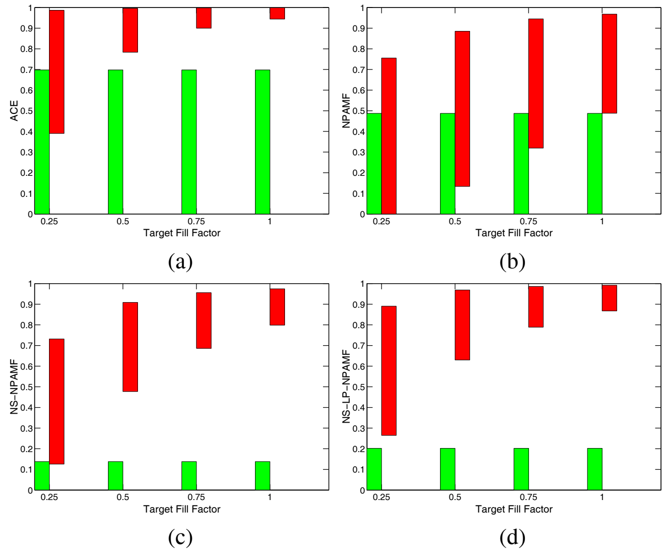

Fig. 2. Test region #1: target-background separation versus target fill factor, where the red (dark) bars correspond to the range of test statistics under H_1, while the green (light) bars show the counterpart under H_0. (a) ACE. (b) NPAMF. (c) NS-NPAMF. (d) NS-LP-NPAMF.

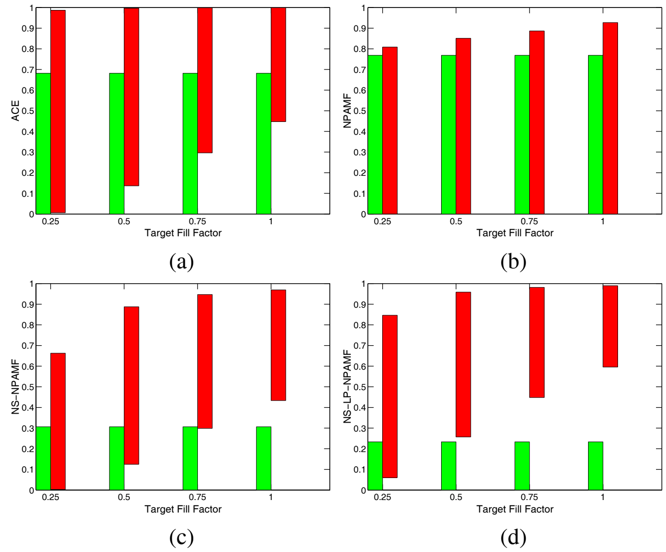

Fig. 3. Test region #2: target-background separation versus target fill factor, where the red (dark) bars correspond to the range of test statistics under H_1, while the green (light) bars show the counterpart under H_0. (a) ACE. (b) NPAMF. (c) NS-NPAMF. (d) NS-LP-NPAMF.

HSI training data. Rather than treating it as an independent process, we cast training screening within the proposed NS-AR framework.

For covariance-matrix based detectors, one screening approach is to use the following metric [9]:

$$T_n = \boldsymbol{x}_n^T \hat{\boldsymbol{R}}_b^{-1} \boldsymbol{x}_n, \quad n = 1, \ldots, N, \tag{12}$$

where $\hat{\boldsymbol{R}}_b$ is the sample covariance matrix obtained from the training pixels. Then, the metric is used to partition the training set $\mathcal{S} \triangleq \{\boldsymbol{x}_1, \ldots, \boldsymbol{x}_N\}$ into two disjoint sets $\mathcal{S}_1$ and $\mathcal{S}_2$ (see [9] for details), of which the former contains the refined training data while the latter contains *outliers* that are discarded.

The above training screening approach relies on an estimate of a full-rank sample covariance matrix $\hat{\boldsymbol{R}}_b$. To circumvent this, we note that $\boldsymbol{x}_n^T \hat{\boldsymbol{R}}_b^{-1} \boldsymbol{x}_n = \|\tilde{\boldsymbol{x}}_n\|^2$, where $\tilde{\boldsymbol{x}} \triangleq \hat{\boldsymbol{R}}_b^{-1/2} \boldsymbol{x}_n$, i.e., the "whitened" version of $\boldsymbol{x}_n$. The whitening operation can be equivalently implemented in a time-series fashion by a whitening filter without the need to estimate $\hat{\boldsymbol{R}}_b$. This alternative screening approach is proposed in [10] and referred to as the *innovation power sorting (IPS)* method, since the output of the whitening filter is often called the *innovation* of the input.

The IPS can be extended and cast within the NS-AR framework. Specifically, we first use the ML estimator in Section III-C to estimate the NS-AR parameters $\{\hat{a}_l(m), \hat{\sigma}_l^2\}$ from the original training set $\mathcal{S}$. Next, we form a shift-varying MA whitening filter from these parameter estimates and, similarly to (3), whiten the training set as follows:

$$\begin{aligned} \breve{x}_n(l) = & \tfrac{1}{\hat{\sigma}_l} \left[x_n(l) + \textstyle\sum_{m=1}^{M} \hat{a}_{l-L_s}(m) x_n(l-m) \right], \\ & l = L_s - 1, \ldots, L-1; \; n = 1, \ldots, N. \end{aligned} \tag{13}$$

Finally, we compute the following metric

$$T_n = \textstyle\sum_{l=L_s-1}^{L-1} \breve{x}_n^2(l), \; n = 1, \ldots, N, \tag{14}$$

which is used to replace (12) for the partition of $\mathcal{S}$ into $\mathcal{S}_1$ and $\mathcal{S}_2$.

IV. Experimental Results

For comparison, we consider the covariance matrix based **ACE** test [2], the AR model based **NPAMF** detector [7] (also see Section III-B), our NS-AR model based **NS-NPAMF** detector (4), and a modified version called **NS-LP-NPAMF** that is briefly explained below. All these detectors use normalized test statistics bounded between 0 and 1, and thus are convenient to compare with. The modification made in the NS-LP-NPAMF detector is due to an observation that HSI spectral data exhibit small oscillations [5]. Such oscillations along the spectral dimension do not contribute much to detection, meanwhile making parameter estimates more noisy. It was found that passing the HSI data through a lowpass (LP) filter to first remove those oscillations before applying the proposed NS-AR modeling, estimation, and detection techniques is helpful. Our NS-NPAMF detector (4) with such a modification is called *NS-LP-NPAMF*.

We use an HSI data set provided in [1]. Fig. 1 is a color infrared (IR) image from a portion of the data set, which shows a view of an airborne hyperspectral data flightline over the Washington DC area. Detailed information on this data set can be found in [1]. Three test regions are highlighted. Test region #1 is relatively homogeneous and formed by grass, test region #2 is less homogeneous with tree and road, and test region #3 corresponds to a heterogeneous environment. To simulate the H_1 condition, we superimpose a target signal to the test pixel. The target signal corresponds to the spectral signature of a man-made object (taken from a pixel in Fig. 1), and is scaled according to particular target fill factors (see [2] for definition of fill factor).

A. Detection in Homogeneous Environments

The figure of merit used is the *separation* of test statistics under H_0 and H_1 [2]. For all methods, we use $N = 8$ training pixels, which corresponds to a 3×3 region without counting the center pixel (i.e., test pixel), for sample covariance matrix or parameter estimation. The sample covariance matrix $\hat{\boldsymbol{R}}_b$ is rank deficient in this case. As suggested in [2], we use the approximation $\hat{\boldsymbol{R}}_b^{-1} \approx \boldsymbol{I} - \boldsymbol{U}_1 \boldsymbol{U}_1^T$, where $\boldsymbol{U}_1$ is formed by the principle eigenvectors of $\hat{\boldsymbol{R}}_b$, for the ACE detector. In this and all other examples, the sliding window length is $L_s = 10$ for NS-NPAMF and NS-LP-NPAMF, and the model order is $M = 5$ selected according to the criterion in Section III-D.

Figs. 2(a) to 2(d) depict the test statistic separation of the four detectors versus the target fill factor for test region #1. As expected,

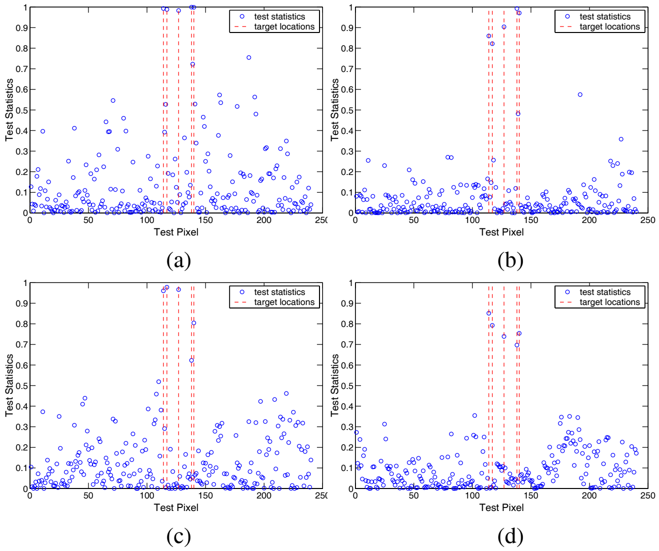

Fig. 4. Test statistics of ACE and NS-LP-NPAMF of test pixels in the test region #3 with 5 embedded targets. (a) ACE without training screening. (b) NS-LP-NPAMF without training screening. (c) ACE with training screening. (d) NS-LP-NPAMF with training screening.

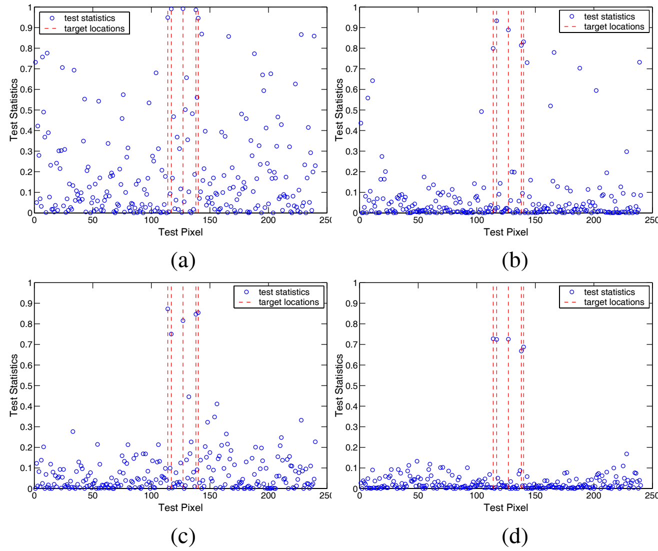

Fig. 5. Test statistics of ACE and NS-LP-NPAMF of test pixels in the test region #1 with 5 embedded targets and more than 20% of the pixels are embedded with outliers. (a) ACE without training screening. (b) NS-LP-NPAMF without training screening. (c) ACE with training screening. (d) NS-LP-NPAMF with training screening.

NPAMF suffers degradation as stationary AR modeling is unsuited for HSI data. Both NS-NPAMF and NS-LP-NPAMF outperform the ACE test, with NS-LP-NPAMF being slightly better than NS-NPAMF. Meanwhile, Figs. 3(a) to 3(d) depict the counterpart results for test region #2, which is less homogeneous than test region #1. It is seen that all four detectors experience some degradation relative to the previous results. However, the proposed NS-NPAMF and NS-LP-NPAMF detectors, especially the latter, still significantly outperform the others.

B. Detection in Heterogeneous Environments

We now consider detection in heterogeneous environments. To this end, we embed 5 targets at randomly chosen locations in test region #3. We run the ACE and NS-LP-NPAMF detectors throughout the test region pixel by pixel, with and without training screening. If training screening is not applied, we use the $N = 8$ pixels surrounding the test pixel for training. Otherwise, we first compute metric (12) for the ACE detector and, respectively, metric (14) for the NS-LP-NPAMF detector using all pixels within the test region, and then the metrics are used to select $N = 8$ new training pixels to refine the parameter/covariance matrix estimate. Figs. 4(a) to 4(d) depict the test statistics of the two detectors, with and without training screening, versus the index of the pixels within the test region. The dotted lines in these plots indicate the indices/locations of the embedded targets. By comparing the results, it is seen that training screening helps both detectors. It is also seen that the proposed NS-LP-NPAMF detector outperforms (i.e., achieves better separation of test statistics under H_0 and H_1) the ACE detector with or without training screening.

Finally, we consider a dense-target scenario by embedding not only 5 targets but also outliers in test region #1. In particular, about 20% of the pixels at random locations in the region are embedded with outliers that have a different spectral signature from that of the target. Figs. 5(a) to 5(d) show the test statistics of the ACE and NS-LP-NPAMF detectors with and without training screening. It is seen that the NS-LP-NPAMF detector overall achieves a better performance than the other.

V. Conclusions

We have developed a class of parametric adaptive detectors by exploiting an NS-AR model for HSI data, and addressed a range of issues including model order selection, training screening, parameter estimation, time-series based signal whitening, and detection. Experimental results show that the proposed parametric detectors are more efficient in training data usage and outperform the covariance-matrix based methods when training is limited.

References

[1] D. A. Landgrebe, *Signal Theory Methods in Multispectral Imaging*, Wiley, Hoboken, NJ, 2003.

[2] D. Manolakis and G. Shaw, "Detection algorithms for hyperspectral imaging applications," *IEEE Signal Processing Magazine*, vol. 19, no. 1, pp. 29–43, January 2002.

[3] M. Rangaswamy and J. H. Michels, "A parametric multichannel detection algorithm for correlated non-gaussian random processes," in *Proceedings of the 1997 IEEE National Radar Conference*, Syracuse, NY, May 1997, pp. 349–354.

[4] J. R. Román, M. Rangaswamy, D. W. Davis, Q. Zhang, B. Himed, and J. H. Michels, "Parametric adaptive matched filter for airborne radar applications," *IEEE Transactions on Aerospace and Electronic Systems*, vol. 36, no. 2, pp. 677–692, April 2000.

[5] H. Li and J. H. Michels, "Parametric adaptive signal detection for hyperspectral imaging," *IEEE Transactions on Signal Processing*, 2006, to appear.

[6] H. Li and J. H. Michels, "Parametric adaptive modeling and detection for hyperspectral imaging," in *Proceedings of the 2004 IEEE International Conference on Acoustics, Speech, and Signal Processing (ICASSP'2004)*, Montreal, Canada, May 2004.

[7] J. H. Michels, et al., "Normalized parametric adaptive matched filter receiver," U.S. Patent No. 6,771,723, issued 3 August 2004.

[8] T. Söderström and P. Stoica, *System Identification*, Prentice Hall International, London, UK, 1989.

[9] P. Chen, W. Melvin, and M. Wicks, "Screening among multivariate normal data," *Journal of Multivariate Analysis*, vol. 69, pp. 10–29, 1999.

[10] J. H. Michels, B. Himed, and M. Rangaswamy, "Robust STAP detection in a dense signal airborne radar environment," *Signal Processing,* special issue on New Trends and Findings in Antenna Array Processing for Radar, vol. 84, pp. 1625–1636, 2004.